Carbon 228 (2024) 119361

Contents lists available at ScienceDirect

Carbon

journal homepage: www.elsevier.com/locate/carbon

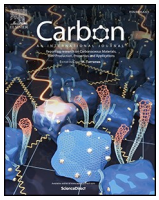

Effect of functional groups on the adsorption of urea on activated carbon

Ruben Asiain-Mira [a,b], Patricia Zamora [b], Victor Monsalvo [b], Laura Torrente-Murciano [a,*]

[a] Department of Chemical Engineering and Biotechnology, University of Cambridge, Philippa Fawcett Drive, CB3 0AS, Cambridge, UK
[b] Aqualia, Department of Innovation and Technology, Avda. Del Camino de Santiago 40, 28050, Madrid, Spain

ARTICLE INFO

Keywords:
Adsorption mechanism
Urea
Urine
Activated carbon
Circular economy

ABSTRACT

The recovery of urea, present in the urine of mammals, has the potential of converting a current wastewater pollutant into an energy source due to its high hydrogen content, in alignment with the waste-to-energy principles. Carbon-based materials enable this approach due to their relatively high urea adsorption capacities. This work reveals that the adsorption of urea from aqueous solutions on activated carbon is a combination of weak van der Waals interactions such hydrogen bonds with the aromatic structure of the pristine carbon surface and also with carboxyl groups on the functionalised carbon, showing no appreciable interaction with hydroxyl or lactone groups. The selective introduction and quantification of different oxygen functional groups on activated carbon reveals their independent effect on the urea adsorption capacity, bringing an end to previous discrepancies in the literature. It also demonstrates that the optimisation of carbon materials must balance the increase of carboxyl groups and the decrease of the surface area associated to functionalisation treatments, providing guidance for future developments of carbon-based materials for circular economy applications.

1. Introduction

Nitrogen is a common pollutant found in urban wastewater that must be removed to avoid eutrophication of water bodies and comply with regulations [1,2]. However, around 80 % of the nitrogen present in urban wastewater comes from the urea ($(NH_2)_2CO$) present in human urine [3], which is a hydrogen rich compound (6.7 wt%) and hence it can be potentially recovered and used as a source of green energy. To facilitate urea recovery from urine, new decentralized wastewater treatment systems must be deployed to treat the urine directly at the production source, where the urea concentration is maximum (20,000 mg L^{-1}) [4–6].

In a recent work, we demonstrated a waste-to-energy strategy where urea is recovered from undiluted urine in decentralized systems to efficiently produce hydrogen as energy carrier to be used in novel energy production methods. For this purpose, a three-steps process was developed, which consisted of i) recovery of urea from urine by adsorption on activated carbon (AC), ii) thermal regeneration of AC and simultaneous decomposition of urea into ammonia, and iii) catalytic decomposition of ammonia to produce hydrogen [7].

In this context, the development of adsorption processes has the potential to selectively recover urea or other valuable compounds from wastewater streams such as urine [8–10]. However, the mechanism of adsorption of urea is not well understood, showing discrepancies between different studies regarding the effect of different functional groups present in AC. Hydroxyl groups are generally associated with urea adsorption on different materials such as chitosan [11] and mesoporous silica [12]. However, hydroxyl groups have also been reported to repulse urea [13]. Some researchers suggest that carboxyl groups have high affinity for urea adsorption, as they can form hydrogen bonds with the amino groups from urea [13]. Other studies claim that urea adsorption takes place through hydrogen bonding of urea with carbonyl groups [13,14], but it is known that urea form chemical bonds with carbonyl groups rather than hydrogen bonds [15]. In conclusion, it is generally accepted that oxygen functional groups on the surface of different adsorbents play an important role on the adsorption of urea. However, there is no consensus on the nature of the functional groups responsible for the adsorption. In addition, there is a lack of quantification of urea adsorption effect of different functional groups on the surface of AC.

In this work, commercial AC is functionalised to introduce different concentrations of hydroxyl, lactone and carboxyl groups on its surface. Adsorption of urea from aqueous solutions is a combination of weak van der Waals interactions such hydrogen bonds with aromatic structure of the pristine AC surface and with carboxyl groups on the functionalised AC, showing no appreciable interaction with hydroxyl or lactone groups.

* Corresponding author.
E-mail address: lt416@cam.ac.uk (L. Torrente-Murciano).

https://doi.org/10.1016/j.carbon.2024.119361
Received 9 February 2024; Received in revised form 14 June 2024; Accepted 15 June 2024
Available online 16 June 2024

Functionalisation of AC is normally associated to a decrease in its surface area, being important to balance it with the introduction of carboxyl groups to maximise urea adsorption capacity.

2. Experimental section

2.1. Functionalisation of activated carbon

Commercial AC with particle size of 50 μm (Supelco) was functionalised using three different oxidising agents, HNO_3 (70 %, Fisher Scientific), H_2SO_4 (98 %, Fisher Scientific), and $KMnO_4$ (98 %, Acros Organics). Solutions of the three oxidising agents at different concentrations (0.2–12 M) were prepared using ultra-high-purified 18.2 MΩ cm Milli-Q water. For the functionalisation process, 10 g of AC were placed in 150 ml of the oxidising agent at certain concentration and the suspension was stirred at different temperatures (60–100 °C) for 3 h under reflux. After functionalisation, the material was filtered and rinsed with distilled water to eliminate the excess acid. The material (10 g) was washed with portions of 200 mL of Milli-Q water up to 10 L, checking that the final pH was constant (4–6). The resulting solid was dried overnight at 80 °C under vacuum.

2.2. Quantification of functional groups

The Boehm titration method was used to quantify the concentration of hydroxyl, lactone and carboxyl groups on commercial and functionalised AC. For this quantification, three portions of 0.5 g of each analysed material were added to 25 mL of NaOH, Na_2CO_3 and $NaHCO_3$ 0.1 M, respectively. The suspensions were magnetically stirred for 24 h and then filtered to remove the AC and aliquots of 10 mL were taken. Each solution was acidified adding 20 mL of HCl 0.1 M except the solution of Na_2CO_3, in which 30 mL were used as it is a diprotic base. The samples were degassed to remove CO_2 by bubbling N_2 for 2 h, following standard recommendations [16]. The solutions were then back-titrated with NaOH 0.1 M using phenolphthalein (indicator, reagent grade, Sigma Aldrich) as endpoint indicator. Solutions were prepared using NaOH (>98 %, Sigma Aldrich), $NaHCO_3$ (>99.5 %, Sigma Aldrich), Na_2CO_3 (>99.5 %, Sigma Aldrich), HCl (1 M, Fisher Scientific) and ultra-high-purified 18.2 MΩ cm Milli-Q water.

The concentrations of hydroxyl, lactone and carboxyl groups were then calculated assuming that $NaHCO_3$ neutralises only carboxyl groups, Na_2CO_3 neutralises carboxyl and lactone groups and NaOH neutralises carboxyl, lactone and hydroxyl groups. Total acid groups were calculated as the sum of hydroxyl, lactone and carboxyl groups. Quantification experiments were carried out in triplicate and the error is the standard deviation of the three experiments.

2.3. Porosity characterisation

N_2 adsorption/desorption analyses were conducted in a Micromeritics ASAP 2020 apparatus whereby ~100 mg of sample was degassed by heating to 110 °C under ultra-high vacuum before the analysis at 77 K. The surface area was calculated according to the Brunauer, Emmett and Teller (BET) method.

2.4. Fourier transform infrared spectroscopy

Fourier transform infrared spectroscopy (FTIR) spectra of carbon materials were acquired in a wavenumber range of 4000–1000 cm^{-1} at room temperature, using a Perkin Elmer FTIR/NIR Frontier spectrophotometer with a zinc selenide crystal equipped with an attenuated total reflectance sampling technique.

2.5. Raman spectroscopy

Raman measurements were performed with a confocal Raman microscope (Renishaw inVia) with a 5x objective lens. A 633 nm excitation source was used with the power set at 10 % to minimise sample damage. For spectra collection, the grating was fixed to 1800 lines mm^{-1}.

2.6. Zeta potential

Zeta potential measurements were recorded on a Malvern Zetasizer Nano ZS instrument equipped with a 633 nm laser. Colloidal suspensions of carbon materials with a concentration of 0.1 mg mL^{-1} were placed in a DTS1070 folded capillary zeta cell for analysis. Three measurements were recorded per samples and the average zeta potential is reported.

2.7. Adsorption experiments

Experiments of urea adsorption were carried out in batch. Urea solutions were prepared using urea (ACS reagent 99.0–100.5 %, Sigma Aldrich) and ultra-high-purified 18.2 MΩ cm Milli-Q water. The experiments were done in vials placed inside a heating block at a constant temperature (30 °C, unless otherwise stated). A given amount of the analysed material was added to an aqueous solution of known concentration of urea under magnetic stirring. After 1 h, to ensure equilibrium is reached, the supernatant was collected by filtration and analysed to determine urea concentration. In the kinetic evaluation, samples were taken at different times from 30 s to 60 min. Unless elsewhere stated, the adsorbent dosage was 40 g L^{-1} and the initial concentration of urea was set at 450 mg L^{-1}.

The concentration of urea in solution was determined using a colorimetric method [17]. 0.5 ml of a colour reagent solution containing 4 % w/v *p*-dimethylaminobenzaldehyde (99 %, Sigma Aldrich) and 4 % v/v sulphuric acid (98 %, Fisher Scientific) in absolute ethanol were added to 2 ml of the urea problem solution. The mixture was stabilized for 30 min and then the absorbance was measured in a spectrophotometer at 430 nm using a blank solution containing 0.5 ml of colour reagent solution and 2 ml of ultra-high-purified 18.2 MΩ cm Milli-Q water.

The amount of urea adsorbed was determined using Eq. (1), assuming that the decrease in the concentration of urea is only due to adsorption.

$$q = \frac{(C_0 - C_f)\,V}{m} \quad \text{Eq. 1}$$

where q (mg g^{-1}) is the amount of urea adsorbed normalised by the adsorbent mass (when equilibrium is reached, it is named as adsorption capacity (q_e)), C_0 and C_f (mg L^{-1}) are the initial and the final concentration of urea in solution respectively, V (mL) is the volume of the solution and m (g) is the mass of adsorbent. When the adsorption capacity is normalised over surface area (Eq. (2)) it is named surface area-adsorption capacity (q_{es}).

$$q_{es} = \frac{q_e}{surface\ area} \quad \text{Eq. 2}$$

All the adsorption experiments were carried out in triplicate and the error is the standard deviation of the three experiments.

2.8. Experimental data fitting

The isotherm data were fit to the Langmuir (Eq. (3)) and Freundlich (Eq. (4)) models to elucidate the mechanism of adsorption [18]. Non-linear fitting was used, so the quality of the fitting was evaluated using the Root Mean Square Error normalised over the range of capacities of each set of experimental data (NRMSE), so they are all comparable (Eq. (5)).

$$q_e = q_m \frac{K_L C_e}{1 + K_L C_e} \quad \text{Eq. 3}$$

$$q_e = K_F C_e^{n_F} \quad \text{Eq. 4}$$

$$NRMSE = \frac{\sqrt{\sum_{i=1}^{n}\left(q_{exp,i} - q_{cal,i}\right)^2}}{q_{max} - q_{min}} \quad \text{Eq. 5}$$

Where q_m (mg g^{-1}) is the monolayer capacity, K_L (L mg^{-1}) and K_F (mg g^{-1} (mg L^{-1})^{nF}) are the equilibrium constant of Langmuir and Freundlich models respectively, n_F is the heterogeneity factor and n is the number of experimental data.

Thermodynamic parameters are estimated using Eq. (6) and Eq. (7).

$$\Delta G^0_{ads} = \Delta H^0_{ads} - T\Delta S^0_{ads} \quad \text{Eq. 6}$$

$$\Delta G^0_{ads} = -RT\ln(K_{ads}) \quad \text{Eq. 7}$$

Where ΔG^0_{ads}, ΔH^0_{ads} and ΔS^0_{ads} are the adsorption Gibbs Free Energy, enthalpy and entropy, respectively, R is the ideal gases constant, T is the adsorption temperature and K_{ads} is the adsorption equilibrium constant.

3. Results and discussion

Commercial AC was functionalised using different oxidising agents to introduce a range of oxygen functional groups on its surface to investigate their independent effect on the urea adsorption capacity. Three different oxidising agents with different concentrations were used to functionalise the AC: nitric acid (1 M, 4 M, 8 M and 12 M); sulphuric acid (1 M, 4 M, 8 M and 12 M); and potassium permanganate (0.2 M). Results of the adsorption capacity (q_e), surface area-adsorption capacity (q_{es}), surface area and concentration of functional groups (hydroxyl, lactone, carboxyl and total) are summarised in Table 1.

Commercial AC presents a low concentration of functional groups, with just ~0.2 mmol g^{-1} of hydroxyl groups. However, commercial AC presents a significant surface area-adsorption capacity of urea of 1.9 mg m^{-2}. This confirms that urea adsorbs on the pristine surface of AC through weak interactions such as Van de Waals or hydrogen bonding, presumably between urea and the delocalised π electrons from the aromatic structure of the carbon [19,20]. This highlights the importance of the AC surface area on the urea adsorption capacity.

Different oxidising agents (nitric acid, sulphuric acid and potassium permanganate) were used to introduce different functional acid groups on the AC surface. As shown in Table 1, the concentration of functional groups generally increases during the oxidising treatment with several factors such the oxidant strength, oxidation temperature and oxidation playing a role on the resulting concentration. The oxidation of the AC surface is known to start on the aliphatic carbons at the edge of the surface or at carbon defects, to follow a sequential oxidation reaction with the initial formation of hydroxyl group, followed by lactone and finally carboxyl groups as depicted in Fig. 1 [21,22].

Acid functionalisation treatment decreases the surface area of the initial commercial AC [23,24]. The surface area decrease might be attributed to a widening in the microporisity, as can be observed in the reduction of the micropore volume together with the surface area reduction (Table S1) [23,24]. It is important to take this factor into consideration during the evaluation of the adsorption capacity and for this reason, surface area-normalised values (q_{es}) are reported in this study.

Fig. 2 shows a clear correlation between the concentration of total acid functional groups and the urea adsorption capacity (q_{es}) of the different AC. The surface area-adsorption capacity increases from $1.9{\cdot}10^{-3}$ mg m^{-2} on the commercial AC up to $2.9{\cdot}10^{-3}$ mg m^{-2} in the case of the AC treated with nitric acid 12 M. This represents an increase of 50 %, indicating that the adsorption on the pristine AC surface dominates, accounting for ~75 % of the urea adsorbed in this case and it is even higher at lower levels of functionalisation. This observation agrees with the fact that correlation in Fig. 2 does not pass through the origin but shows a y-axis intercept of $1.8{\cdot}10^{-3}$ mg m^{-2}, which represents the extension of adsorption associated to the pristine surface area of the AC rather than to acid functional groups.

As different oxidising agents, concentrations and temperatures lead to different functionalised AC, the data in Table 1 reveals fundamental information about the effect of the nature of the functional groups on the urea adsorption capacity. Increasing the concentration of nitric acid during functionalisation results on an increase in the concentration of lactone and carboxyl groups [25,26]. There is also an increase in the concentration hydroxyl groups, although no clear trend is observed with respect to the nitric acid concentration. Nitric acid is generally accepted as the best wet oxidant for introducing oxygen functional groups on AC [22,27]. Nitric acid treatment also reduces the AC surface area, more significantly with increasing concentration. Despite this, the urea surface area-adsorption capacity clearly increases as the total acid group concentration increases, demonstrating the importance of carboxyl and/or lactone groups, rather than hydroxyl ones in the urea adsorption capacity. These results are in good agreement with the interaction of urea with functional groups in proteins, where the hydrogen bonding of carboxylic oxygen with urea is stronger than hydrogen bonding with hydroxyl groups [19].

Treatment of AC with potassium permanganate results on a minimum concentration of carboxyl groups close to zero, similar to the commercial AC. However, the concentration of hydroxyl, and specially lactone, groups increase significantly. Although potassium permanganate is a strong oxidiser, the low concentration (0.2 M) used in this treatment might to be responsible of the partial oxidation of the AC, not achieving the formation of carboxyl groups as it happens with nitric and

Table 1
Quantification of functional groups of AC before and after functionalisation process and their adsorption capacities.

Treatment	q_e (mg g^{-1})	Surface area (m^2 g^{-1})	q_{es} (mg m^{-2})	Hydroxyl (mmol g^{-1})	Lactone (mmol g^{-1})	Carboxyl (mmol g^{-1})	Total acid (mmol g^{-1})
Commercial	1.8 ± 0.1	940	1.9 ± 0.2	0.17	0.01	0.05	0.23
HNO_3 1 M – 60 °C	1.7 ± 0.1	890	1.9 ± 0.2	0.30	0.01	0.20	0.51
HNO_3 1 M	2.2 ± 0.1	890	2.5 ± 0.1	0.46	0.16	0.44	1.06
HNO_3 4 M	2.1 ± 0.1	863	2.5 ± 0.2	0.36	0.49	0.54	1.39
HNO_3 8 M	2.2 ± 0.1	785	2.8 ± 0.1	0.56	0.54	0.69	1.79
HNO_3 1 M – 100 °C	2.1 ± 0.1	850	2.5 ± 0.2	0.90	0.34	0.70	1.94
HNO_3 12 M	2.3 ± 0.1	798	2.9 ± 0.2	0.38	0.64	1.02	2.04
H_2SO_4 1 M	1.8 ± 0.3	934	2.0 ± 0.3	0.06	0.14	0.10	0.30
H_2SO_4 4 M	1.8 ± 0.1	948	1.9 ± 0.2	0.06	0.29	0.10	0.45
H_2SO_4 8 M	1.8 ± 0.2	921	2.0 ± 0.2	0.11	0.29	0.10	0.50
H_2SO_4 12 M	1.8 ± 0.1	796	2.3 ± 0.2	0.06	0.34	0.15	0.55
$KMnO_4$ 0.2 M	1.5 ± 0.3	705	2.1 ± 0.4	0.36	0.37	0.01	0.74

Experimental conditions during functionalisation: AC mass: 10 g, oxidiser volume: 150 mL, T = 80 °C (unless specifically stated differently) under reflux, t = 3 h.
Functional groups concentration error:± 0.1 mmol g^{-1}.
Experimental conditions during adsorption experiments: C_0 = 450 mg L^{-1}, T = 30 °C, t = 1 h, adsorbent dosage: 40 g L^{-1}.

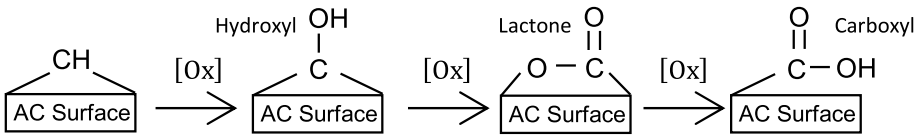

Fig. 1. Sequence of the oxidation reaction of the AC surface during functionalisation [21,22].

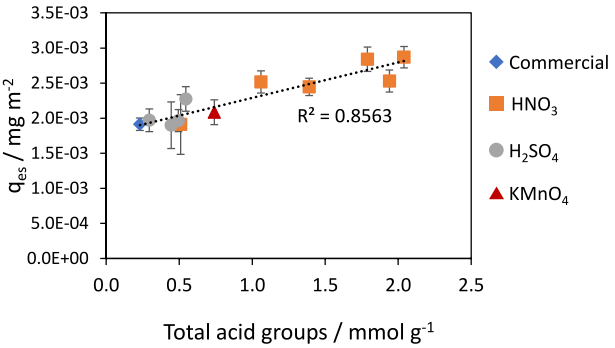

Fig. 2. Correlation between the surface area normalised adsorption capacity and the concentration of total acid functional groups of the AC.

sulphuric acids [28]. However, the treatment with potassium permanganate is the most aggressive in terms of surface area reduction. As surface area-adsorption capacity does not show a significant change between commercial and $KMnO_4$-treated AC, it can be inferred that lactone groups do not play a significant role on the adsorption of urea. As a result, it can be concluded that carboxyl groups are the most active from the three acid groups evaluated towards adsorption of urea.

Finally, as can be observed in Table 1, treatment of AC with sulphuric acid introduces a lower amount of functional groups – mainly lactone – than nitric acid or potassium permanganate [29]. The surface area-adsorption capacity does not significantly change with increasing concentration of sulphuric acid during the treatment despite the increase on the lactone groups, supporting the fact that lactone groups show low affinity towards urea.

FTIR spectra of commercial and functionalised activated carbon materials show very little differences (Fig. S3. A), expected due to the low concentration of functional groups as quantified in Table 1. At 1600 cm^{-1}, a peak appears in the functionalised materials which is attributed to the C═O stretching vibration caused by the increase in the lactone and carboxyl groups [30].

Raman spectra of the activated carbon materials show two bands at 1350 (D band) and 1590 cm^{-1} (G band) (Fig. S3. B). The first peak corresponds to the vibrations of the sp^3-bonded carbon atoms of defects and disorder, while the latter is attributed to the sp^2-bonded carbon atoms in a hexagonal graphitic ring [31]. The D/G intensity ratio increases with the functionalisation of the activated carbon, especially for the material treated with $KMnO_4$. This implies an increase in the amorphous degree of the activated carbon after the treatment [32].

The zeta potential of the functionalised activated carbon materials (Fig. S4) show negative values due to their negatively charged surface associated to the delocalised π electrons and oxygen, especially carboxyl, functional groups [33].

Furthermore, the effect of the functionalisation temperature was evaluated between 60 and 100 °C for the treatment of AC with acid nitric (1 M). Increasing temperatures led to a higher presence of the three types of functional groups (Table 1). However, the surface area decreases more significantly with increasing temperature, which overcomes the positive effect of the functional groups. Therefore, out of the treatments evaluated, the AC functionalised with HNO_3 1 M at 80 °C is found to be optimum for urea adsorption, balancing the introduction of carboxyl groups and the reduction of the surface area.

The adsorption mechanism of urea onto AC is a combination of weak van der Waals interactions, such hydrogen bonding, between the amino groups of urea with i) delocalised π electrons of the aromatic structure of the AC and ii) carboxyl groups. The adsorption mechanism is represented in Fig. 3. Urea has a dipole moment of 4.5 D [34] while water just have 1.8 D [35]. The higher polarity may explain the preferential adsorption of urea in high electron density sites, such as π electrons of aromatic carbon rings and carboxyl groups (which present a resonant structure of the double bond). This fundamental understanding provides guidelines for the development of new materials with enhanced urea adsorption capacity.

To get further information about the adsorption of urea on the surface of AC and the carboxyl groups, commercial and functionalised AC (HNO_3 1 M 80 °C) were compared. Fig. 4 shows the adsorption isotherms at 30, 45 and 60 °C using both materials.

In both materials, the adsorption capacity for a given equilibrium concentration increases as the temperature decreases, which confirms the overall exothermic nature of adsorption processes [36]. Both commercial and functionalised AC show a linear relationship between the amount of urea adsorbed (q_e) and the concentration of urea in the solution (C_e) under equilibrium conditions at low concentration values. This relationship plateaus slightly at higher concentrations and, although the amount of urea adsorbed is higher in the latter case, full saturation is not achieved in any materials. This suggests a low affinity between urea and AC, which could be related to the similar molecular properties of water and urea and the difficulty to separate them [37]. Isotherm data are fitted to Langmuir and Freundlich models (Eq. (4) and Eq. (5)) to evaluate if the adsorption occurs in a monolayer or in multilayer. The fitting parameters and the NRMSE are summarised in Table 2.

The Langmuir model assumes monolayer adsorption while Freundlich model considers that adsorption can happen on multilayers [36]. As can be observed in Table 2, both models show similar fittings, with comparable NRMSE values and n_F values < 1 which confirms that the adsorption of urea on activated carbon takes place in a monolayer for the range of urea concentrations studied [7]. The values of the monolayer capacity q_m, are higher for the functionalised AC than for the commercial one, confirming the higher adsorption performance of the carboxyl groups compared to AC surface itself. As previously found [7], the adsorption capacity of the activated carbons studied in this work is in the low range of previous carbon-based materials previously reported in the literature, with capacities ranging between 1.1 and 877.9 mg g^{-1} (Table S 2), being difficult to identify the reasons behind the differences [8,13,14,38–40].

Thermodynamic parameters are calculated using Eq. (6) and Eq. (7). For uncharged adsorbates as urea, the equilibrium constant of adsorption (K_{ads}) can be reasonably approximated by the Langmuir equilibrium constant (K_L) [41] and used in Eq. (6) to obtain the Gibbs Free Energy at each studied temperature (Table 3). As expected, all Gibbs Free Energies present negative values, as the adsorption is a spontaneous process under tests conditions. As the Langmuir equilibrium constant is higher for the commercial AC, higher Gibbs free energy values are obtained in the functionalised AC, with no particular physical meaning. A linear fitting of the Gibbs Free Energy values against temperature provides the enthalpy and entropy of adsorption values according to Eq. (7). The fitting is shown in Fig. 5 and the results ae summarised in Table 3.

As can be observed in Table 3, the enthalpy and entropy values of urea adsorption are similar for the commercial and functionalised AC as

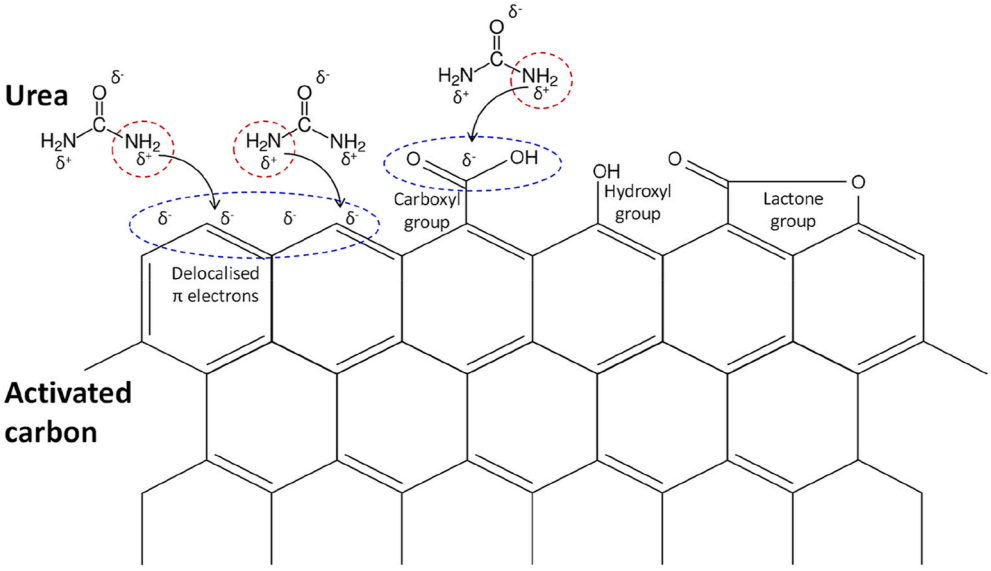

Fig. 3. Scheme of the adsorption mechanism of urea onto AC.

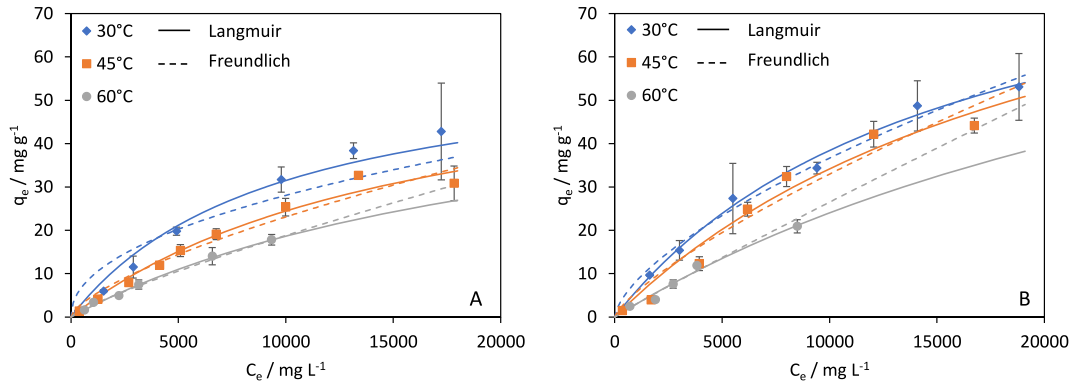

Fig. 4. Isotherm experimental data and Langmuir and Freundlich fittings for adsorption of urea onto activated carbon at different temperatures. A: Commercial activated carbon. B: Functionalised activated carbon (HNO_3 1 M 80 °C).

Table 2
Langmuir fitting parameters for the isotherms of adsorption of urea onto commercial and functionalised AC.

Parameter	Commercial AC			Functionalised AC		
	30°C	45°C	60°C	30°C	45°C	60°C
Langmuir						
q_m (mg g^{-1})	62	64	61	98	110	109
K_L (L mg^{-1})·10^5	10.5	6.2	4.4	6.5	4.5	2.8
NRMSE	0.062	0.050	0.024	0.036	0.072	0.049
Freundlich						
K_F (mg g^{-1} (mg L^{-1})^{nF})	0.370	0.044	0.009	0.094	0.030	0.004
n_F	0.47	0.68	0.83	0.65	0.76	0.95
NRMSE	0.123	0.064	0.025	0.047	0.089	0.063

Functionalisation conditions: HNO_3 1 M 80 °C.

expected due to the similar interactions of urea with the AC surface and the carboxyl groups as discussed above. Enthalpies values are negative, due to the exothermicity of the adsorption process, favoured at low temperatures, in agreement with the isotherm data abovementioned. Their low values (<50 kJ/mol) indicates that the process is driven by physisorption mechanism [36], as expected by weak van der Waals interactions such hydrogen bonds. The entropy values are also negative, meaning that the adsorption process involves a decrease in the degrees of freedom of the system as a result of the immobilization of the adsorbate on the surface of the adsorbent [36].

Regarding adsorption kinetics, despite the differences between the commercial and functionalised AC, urea adsorption is extremely fast in both materials, reaching equilibrium within the first sampling interval of 30 s (Fig. 6). More time resolution would be necessary for extracting conclusions on the limiting step. In previous works, using activated AC in the form of pellets of 0.8 mm particle size, it was determined that intraparticle diffusion (internal mass transfer) was the limiting step [7], which may not be possible to observe in this case due to the very small granulometry of the AC used in this work (50 μm) which significantly reduces the internal mass transfer resistance. This fast kinetic process has important positive implications for the deployment of these materials in full-scale adsorption systems. In addition, the weak interactions of urea with the AC surface and carboxylic groups suggest that the AC might be easily regenerated. Our previous work with commercial activated carbon showed that a thermal treatment was efficient for the regeneration of the material, and its use on consecutive adsorption/-desorption cycles which can be now correlated with weak physical adsorption [7].

4. Conclusions

In this paper, we demonstrate the relationship between the nature of

Table 3
Langmuir equilibrium constant and Gibbs Free Energy for adsorption isotherm at different temperatures.

	Commercial AC				Functionalised AC			
T (°C)	K_L (L mol^{-1})	ΔG° (kJ mol^{-1})	ΔH° (kJ mol^{-1})	ΔS° (J mol^{-1})	K_L (L mol^{-1})	ΔG° (kJ mol^{-1})	ΔH° (kJ mol^{-1})	ΔS° (J mol^{-1})
30	6.3	−4.6	−24.2	−64.9	3.9	−3.4	−23.1	−64.8
45	3.7	−3.5			2.7	−2.6		
60	2.6	−2.7			1.7	−1.5		

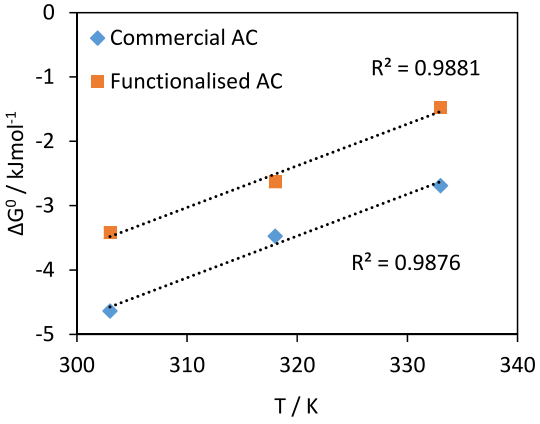

Fig. 5. Gibbs Free Energy against temperature for adsorption of urea onto commercial and functionalised (HNO_3 1 M 80 °C) AC.

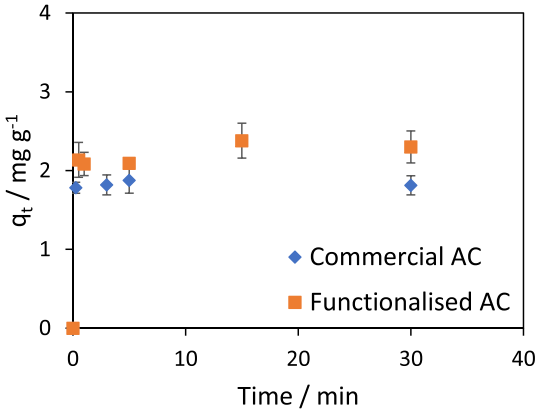

Fig. 6. Kinetic study of the adsorption of urea onto commercial and functionalised (HNO_3 1 M 80 °C) AC. C_0 = 450 mg L^{-1}; Adsorbent dosage = 40 g L^{-1}; T = 30 °C.

oxygen containing functional groups in activated carbon and their effect on the adsorption capacity of urea. For this, hydroxyl, lactone and carboxyl groups are introduced and quantified on the surface of activated carbon using different oxidising agents: nitric acid, sulphuric acid and potassium permanganate. The results show that pristine unfunctionalised activated carbon adsorbs urea through its hydrogen bonding with delocalised π electrons of the carbon's aromatic structure. A similar mechanism of adsorption is observed in presence of carboxyl groups, but not with hydroxyl or lactone groups. Surface area and surface groups exert a significant impact on the adsorption capacity, which must be balanced by means of maximising the presence of carboxyl groups and avoiding the reduction of surface area. In addition, the thermodynamic analysis suggests that urea adsorption on the materials tested takes place in a monolayer driven by physisorption, with very high adsorption rates. This work provides understanding to guide the design of new adsorption materials with enhanced urea adsorption capacity which should aim to maximise their surface area and concentration of hydroxyl groups. Despite the potential of carbon-based materials to recover urea from urine as nutrient recovery or energy source, it is important to point out that this work has been carried out using ideal urea solutions and thus further studies should be carried out with real urine samples to understand interferences in the adsorption process.

CRediT authorship contribution statement

Ruben Asiain-Mira: Writing – original draft. **Patricia Zamora:** Writing – review & editing. **Victor Monsalvo:** Writing – review & editing. **Laura Torrente-Murciano:** Writing – review & editing.

Declaration of competing interest

The authors declare the following financial interests/personal relationships which may be considered as potential competing interests:

Laura Torrente Murciano reports financial support was provided by EU Framework Programme for Research and Innovation Marie Sklodowska-Curie Actions. If there are other authors, they declare that they have no known competing financial interests or personal relationships that could have appeared to influence the work reported in this paper.

Acknowledgements

The authors greatly acknowledge the financial support from the European Union's Horizon 2020 research and innovation programme in the frame of REWATERGY, Sustainable Reactor Engineering for Applications on the Water-Energy Nexus, MSCA-ITN-EID Project N. 812574. For the purpose of open access, the author has applied a Creative Commons Attribution (CC BY) licence to any Author Accepted Manuscript version arising from this submission. The authors acknowledge the support of staff from Lleida WWTP (J. Palatsi and M.S. Romero-Güiza). The authors acknowledge T. Hussein and B. Pinho from University of Cambridge their support with the analyses.

Appendix A. Supplementary data

Supplementary data to this article can be found online at https://doi.org/10.1016/j.carbon.2024.119361.

References

[1] W. Zhang, R. Fu, L. Wang, J. Zhu, J. Feng, W. Yan, Rapid removal of ammonia nitrogen in low-concentration from wastewater by amorphous sodium titanate nano-particles, Sci. Total Environ. (2019), https://doi.org/10.1016/j.scitotenv.2019.03.051.
[2] M.S. Romero-Güiza, X. Flotats, R. Asiain-Mira, J. Palatsi, Enhancement of sewage sludge thickening and energy self-sufficiency with advanced process control tools in a full-scale wastewater treatment plant, Water Res. 222 (2022) 118924, https://doi.org/10.1016/j.watres.2022.118924.
[3] L. Egle, H. Rechberger, M. Zessner, Overview and description of technologies for recovering phosphorus from municipal wastewater, Resour. Conserv. Recycl. 105 (2015) 325–346, https://doi.org/10.1016/j.resconrec.2015.09.016.
[4] D.F. Putnam, Composition and Concentrative Properties of Human Urine, Huntington Beach, California, 1971.
[5] D. Weerakoon, B. Bansal, L.P. Padhye, A. Rachmani, L. James Wright, G. Silyn Roberts, S. Baroutian, A critical review on current urea removal technologies from

water: an approach for pollution prevention and resource recovery, Sep. Purif. Technol. 314 (2023) 123652, https://doi.org/10.1016/j.seppur.2023.123652.
[6] C. Rose, A. Parker, B. Jefferson, E. Cartmell, The characterization of feces and urine: a review of the literature to inform advanced treatment technology, Crit. Rev. Environ. Sci. Technol. 45 (2015) 1827–1879, https://doi.org/10.1080/10643389.2014.1000761.
[7] R. Asiain-Mira, C. Smith, P. Zamora, V.M. Monsalvo, L. Torrente-Murciano, Hydrogen production from urea in human urine using segregated systems, Water Res. 222 (2022) 118931, https://doi.org/10.1016/j.watres.2022.118931.
[8] M. Ganesapillai, P. Simha, A. Zabaniotou, Closed-loop fertility cycle: realizing sustainability in sanitation and agricultural production through the design and implementation of nutrient recovery systems for human urine, Sustain. Prod. Consum. 4 (2015) 36–46, https://doi.org/10.1016/j.spc.2015.08.004.
[9] M.A. Maia, G.L. Dotto, O.W. Perez-Lopez, M. Gutterres, Phosphate removal from industrial wastewaters using layered double hydroxides, Environ. Technol. 42 (2021) 3095–3105, https://doi.org/10.1080/09593330.2020.1722257.
[10] M. Avena Maia, O.P. Kranse, S. Eves-Van Den Akker, L. Torrente-Murciano, Phosphate recovery from urine-equivalent solutions for fertilizer production for plant growth, ACS Sustain. Chem. Eng. 11 (2023) 16074–16086, https://doi.org/10.1021/acssuschemeng.3c03146.
[11] C. Xue, L.D. Wilson, Kinetic study on urea uptake with chitosan based sorbent materials, Carbohydr. Polym. 135 (2016) 180–186, https://doi.org/10.1016/j.carbpol.2015.08.090.
[12] W.K. Cheah, Y.L. Sim, F.Y. Yeoh, Amine-functionalized mesoporous silica for urea adsorption, Mater. Chem. Phys. 175 (2016) 151–157, https://doi.org/10.1016/j.matchemphys.2016.03.007.
[13] C.H. Ooi, W.K. Cheah, Y.L. Sim, S.Y. Pung, F.Y. Yeoh, Conversion and characterization of activated carbon fiber derived from palm empty fruit bunch waste and its kinetic study on urea adsorption, J. Environ. Manag. 197 (2017) 199–205, https://doi.org/10.1016/j.jenvman.2017.03.083.
[14] T. Kameda, S. Ito, T. Yoshioka, Kinetic and equilibrium studies of urea adsorption onto activated carbon: adsorption mechanism, J. Dispersion Sci. Technol. 38 (2017) 1063–1066, https://doi.org/10.1080/01932691.2016.1219953.
[15] M.N.Z. Abidin, P.S. Goh, A.F. Ismail, N. Said, M.H.D. Othman, H. Hasbullah, M. S. Abdullah, B.C. Ng, S.H.S.A. Kadir, F. Kamal, Highly adsorptive oxidized starch nanoparticles for efficient urea removal, Carbohydr. Polym. 201 (2018) 257–263, https://doi.org/10.1016/j.carbpol.2018.08.069.
[16] S.L. Goertzen, K.D. Thériault, A.M. Oickle, A.C. Tarasuk, H.A. Andreas, Standardization of the Boehm titration. Part I. CO2 expulsion and endpoint determination, Carbon N Y (2010), https://doi.org/10.1016/j.carbon.2009.11.050.
[17] C.J. Andersen, B. Strange, Colorimetric determination of urea, Scand. J. Clin. Lab. Invest. 11 (1959) 122–127, https://doi.org/10.3109/00365515909060419.
[18] K.Y. Foo, B.H. Hameed, Insights into the modeling of adsorption isotherm systems, Chem. Eng. J. 156 (2010) 2–10, https://doi.org/10.1016/j.cej.2009.09.013.
[19] E.J. Guinn, L.M. Pegram, M.W. Capp, M.N. Pollock, M.T. Record, Quantifying why urea is a protein denaturant, whereas glycine betaine is a protein stabilizer, Proc. Natl. Acad. Sci. U. S. A. 108 (2011) 16932–16937, https://doi.org/10.1073/pnas.1109372108.
[20] V. Bernal, L. Giraldo, J. Moreno-Piraján, Physicochemical properties of activated carbon: their effect on the adsorption of pharmaceutical compounds and adsorbate–adsorbent interactions, C (Basel) 4 (2018) 62, https://doi.org/10.3390/c4040062.
[21] C.L. Mangun, K.R. Benak, M.A. Daley, J. Economy, Oxidation of activated carbon fibers: effect on pore size, surface chemistry, and adsorption properties, Chem. Mater. 11 (1999) 3476–3483, https://doi.org/10.1021/cm990123m.
[22] W.M.A.W. Daud, A.H. Houshamnd, Textural characteristics, surface chemistry and oxidation of activated carbon, J. Nat. Gas Chem. 19 (2010) 267–279, https://doi.org/10.1016/S1003-9953(09)60066-9.
[23] L.J. Lemus-Yegres, I. Such-Basáñez, M.C. Román-Martínez, C.S.M. de Lecea, Catalytic properties of a Rh-diamine complex anchored on activated carbon: effect of different surface oxygen groups, Appl. Catal. Gen. 331 (2007) 26–33, https://doi.org/10.1016/j.apcata.2007.07.020.
[24] C. Moreno-Castilla, M.A. Ferro-García, J.P. Joly, I. Bautista-Toledo, F. Carrasco-Marín, J. Rivera-Utrilla, Activated carbon surface modifications by nitric acid, hydrogen peroxide, and ammonium peroxydisulfate treatmenss, Langmuir 11 (1995) 4386–4392, https://doi.org/10.1021/la00011a035.
[25] C. Aguilar, R. García, G. Soto-Garrido, R. Arriagada, Catalytic wet air oxidation of aqueous ammonia with activated carbon, Appl. Catal., B 46 (2003) 229–237, https://doi.org/10.1016/S0926-3373(03)00229-7.
[26] P. Chingombe, B. Saha, R.J. Wakeman, Surface modification and characterisation of a coal-based activated carbon, Carbon N Y 43 (2005) 3132–3143, https://doi.org/10.1016/j.carbon.2005.06.021.
[27] C. Moreno-Castilla, M.V. López-Ramón, F. Carrasco-Marín, Changes in surface chemistry of activated carbons by wet oxidation, Carbon N Y 38 (2000) 1995–2001, https://doi.org/10.1016/S0008-6223(00)00048-8.
[28] A.A.M. Daifullah, S.M. Yakout, S.A. Elreefy, Adsorption of fluoride in aqueous solutions using KMnO4-modified activated carbon derived from steam pyrolysis of rice straw, J. Hazard Mater. 147 (2007) 633–643, https://doi.org/10.1016/j.jhazmat.2007.01.062.
[29] H.T. Gomes, S.M. Miranda, M.J. Sampaio, A.M.T. Silva, J.L. Faria, Activated carbons treated with sulphuric acid: catalysts for catalytic wet peroxide oxidation, Catal. Today 151 (2010) 153–158, https://doi.org/10.1016/j.cattod.2010.01.017.
[30] R. Ali, Z. Aslam, R.A. Shawabkeh, A. Asghar, I.A. Hussein, BET, FTIR, and Raman characterizations of activated carbon from waste oil fly ash, Turk. J. Chem. 44 (2020) 279–295, https://doi.org/10.3906/KIM-1909-20.
[31] Z. Wei, R. Pan, Y. Hou, Y. Yang, Y. Liu, Graphene-supported Pd catalyst for highly selective hydrogenation of resorcinol to 1, 3-cyclohexanedione through giant π-conjugate interactions, Sci. Rep. 5 (2015), https://doi.org/10.1038/srep15664.
[32] S. Mopoung, N. Dejang, Activated carbon preparation from eucalyptus wood chips using continuous carbonization–steam activation process in a batch intermittent rotary kiln, Sci. Rep. 11 (2021), https://doi.org/10.1038/s41598-021-93249-x.
[33] M. Dai, The effect of zeta potential of activated carbon on the adsorption of dyes from aqueous solution: I. The adsorption of cationic dyes: methyl green and methyl violet, J. Colloid Interface Sci. 164 (1994) 223–228, https://doi.org/10.1006/jcis.1994.1160.
[34] W.R. Gilkerson, K.K. Srivastava, The dipole moment of urea, J. Phys. Chem. 64 (1960) 1485–1487, https://doi.org/10.1021/j100839a032.
[35] T. Zhu, T. Van Voorhis, Understanding the dipole moment of liquid water from a self-attractive hartree decomposition, J. Phys. Chem. Lett. 12 (2021) 6–12, https://doi.org/10.1021/acs.jpclett.0c03300.
[36] E. Worch, Adsorption Technology in Water Treatment: Fundamentals, Processes and Modeling, De Gruyter, 2012, https://doi.org/10.1515/9783110240238.
[37] H.D. Lehmann, R. Marten, C.A. Gullberg, How to catch urea? Considerations on urea removal from hemofiltrate, Artif. Organs 5 (1981) 278–285, https://doi.org/10.1111/j.1525-1594.1981.tb04002.x.
[38] S.M. Safwat, M.E. Matta, Adsorption of urea onto granular activated alumina: a comparative study with granular activated carbon, J. Dispersion Sci. Technol. 39 (2018) 1699–1709, https://doi.org/10.1080/01932691.2018.1461644.
[39] M. Ganesapillai, P. Simha, The rationale for alternative fertilization: equilibrium isotherm, kinetics and mass transfer analysis for urea-nitrogen adsorption from cow urine, Resource-Efficient Technologies (2015), https://doi.org/10.1016/j.reffit.2015.11.001.
[40] Y.C. Cheng, C.C. Fu, Y.S. Hsiao, C.C. Chien, R.S. Juang, Clearance of low molecular-weight uremic toxins p-cresol, creatinine, and urea from simulated serum by adsorption, J. Mol. Liq. 252 (2018) 203–210, https://doi.org/10.1016/j.molliq.2017.12.084.
[41] Y. Liu, Is the Free Energy Change of Adsorption Correctly Calculated? J Chem Eng Data, 2009, pp. 1981–1985, https://doi.org/10.1021/je800661q.